Silent Satellites: Critical Fluctuations in Chromiun

B. J. Sternlieb, J. P. Hill, T. Inami, and G. Shirane
Physics Department, Brookhaven National Laboratory, Upton, New York 11973

W.-T. Lee and S. A. Werner
Department of Physics, University of Missouri, Columbia, Missouri 65211

Eric Fawcett
Department of Physics, University of Toronto, Toronto, Canada M5S 1A7
(Received 31 October 1994)

Neutron scattering measurements of critical fluctuations associated with the spin-density-wave transition at the Néel temperature $T_N = 311$ K, in a single-**Q** chromium crystal are reported. Surprisingly, critical fluctuations are observed emanating from satellite positions, corresponding to *absent* magnetic domains, at which no elastic scattering occurs. The inelastic scattering from these "silent satellites" grows rapidly with increasing temperature, becoming equal to the allowed single-**Q** satellite scattering at T_N.

PACS numbers: 75.30.Fv, 75.40.Gb

The disappearance of the long-range ordered, spin-density-wave (SDW) state of pure chromium at the Néel temperature, $T_N \approx 311$ K, was first recognized to be weakly first order by Arrott, Werner, and Kendrick [1] 30 years ago. Single-**Q** magnetic domain samples can be produced by cooling through T_N with a large magnetic field aligned along the [100] crystal axis. After removing the field, the resulting ordered phase, at temperatures below T_N but above the spin flip transition at $T_{\mathrm{SF}} = 122$ K, is a magnetically orthorhombic, transversely polarized SDW state characterized by the incommensurate magnetic satellites at $\mathbf{Q}_{\pm} = (1 \pm \delta, 0, 0)$. Observation of the critical fluctuations leading to the disappearance of this SDW phase and the return of cubic symmetry in the paramagnetic state have largely eluded all previous experiments [2–4]. The principle result of this Letter is the observation of critical scattering emanating not only from the allowed, incommensurate elastic magnetic satellites of the underlying ordered phase but also from satellites, $\mathbf{Q}_{\pm}^{s} = \{(1, \pm\delta, 0)\&(1, 0, \pm\delta)\}$, at which no static magnetic scattering exists. In addition, the **q** width of this scattering demonstrates an unusually weak temperature dependence. We know of no other system in which such purely dynamic "silent satellite" scattering has been observed. On the other hand, like chromium, other itinerant systems evincing incommensurate charge-density or spin-density instabilities, as originally discussed by Overhauser [5], might prove accessible to similar studies. The existence of these silent satellite fluctuations leads, for the first time, to a consistent picture of the symmetry change at the Néel transition in chromium and provides a unique opportunity to study critical fluctuations in an ordered state without an attendant underlying static magnetization wave.

The measurements presented below were performed at the HFBR H-9 triple-axis spectrometer using a $60'$-$40'$-$60'$-S-$80'$-$80'$ collimation configuration and unpolarized neutrons with a fixed incident energy of $E_i = 5.0$ meV. The (002) reflection of pyrolytic graphite was used to monochromate and analyze the incident and scattered neutrons. Cold beryllium was used to filter higher order (λ/n) contamination from the incident beam. Two crystals were used for the measurements: Cr#10, an irregularly shaped 25.6 g single crystal with a 0.73° mosaic and Cr-f, and a rectangular, $6.2 \times 5.9 \times 7.0$ mm^3, 1.9 g single crystal with a 0.48° mosaic. Prior to the measurements, each sample was prepared in a single domain or single-**Q** magnetic state by cooling through Néel transition to room temperature with a magnetic field of $|\mathbf{H}| = 20$ T applied along the $(h00)$ crystal axis [6]. After removing the field, the samples were mounted in separate, closed cycle ^{4}He refrigerators with the $(00l)$ axis normal to the scattering plane. Two sets of satellites are accessible in this geometry: the $(1 \pm \delta, 0, 0)$ and $(\pm\delta, 1, 0)$ satellites, corresponding to the allowed magnetic reflections of the prepared single-**Q** state, and the $(0, 1 \pm \delta, 0)$ and $(1, \pm\delta, 0)$ silent satellites of the absent $\mathbf{Q}_{\pm}^{y} = (0, 1 \pm \delta, 0)$ magnetic domain (Fig. 2, inset). Before the scattering experiments, both crystals were cooled to a temperature of $T = 250$ K. All subsequent elastic and inelastic measurements were made with monotonically increasing temperature.

Our central result is presented in the $T = 307$ K, Cr#10 data of Fig. 1. The $\Delta E = 0$ scans in the top panel of the figure show that elastic scattering from the silent satellite positions is almost completely absent. The measured ratio of allowed to silent satellite elastic intensities, i.e., the single-**Q** ratio, is $\gtrsim 1000{:}1$. The absence of elastic silent satellite scattering contrasts sharply with the inelastic intensities observed at $\Delta E = 0.5$ meV, shown in the bottom panel. These data indicate that strong fluctuations are simultaneously present at *both* the allowed and silent satellites. The assignment of a purely

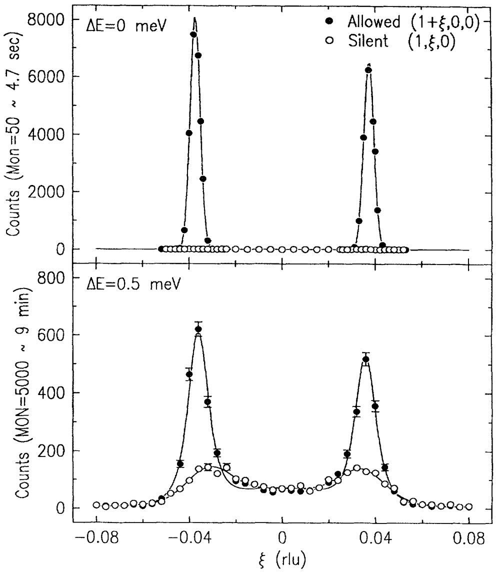

FIG. 1. Top: elastic scans in Cr#10 at allowed (●) and silent (○) satellite positions at $T = 307$ K. Bottom: equivalent inelastic scans with $\Delta E = 0.5$ meV, which demonstrate the existence of fluctuations at *both* allowed and silent satellite positions.

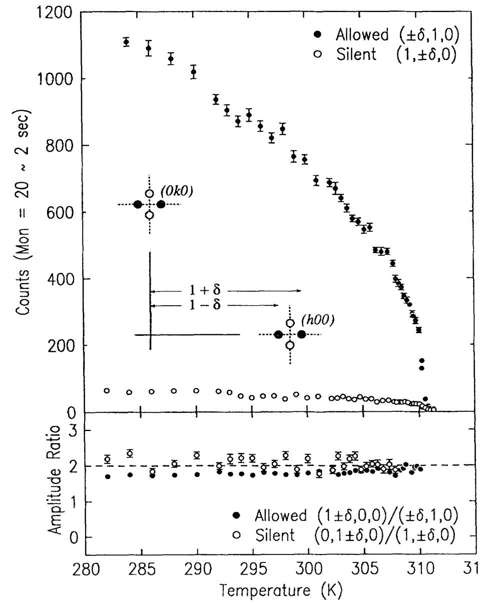

FIG. 2. Temperature dependence of the elastic scattering intensity for Cr-f. Inset: ($hk0$) scattering plane with accessible silent (○) and allowed (●) satellites. Top: elastic scattering intensities from transverse scans through the allowed $(\pm\delta, 1, 0)$ and silent $(1, \pm\delta, 0)$ satellites. Bottom: longitudinal/transverse intensity ratios with the ideal value $\mathcal{R}_{\rm elastic}$ shown by a dashed line.

magnetic character to these peaks is straightforward as the phonon spectrum of chromium is largely uneffected by the Néel transition [7], and the weak nuclear scattering associated with the finite charge-density-wave below T_N is observed only about the allowed nuclear reflections with an incommensurate offset twice that of the magnetic fundamental, i.e., $(2 \pm 2\delta, 0, 0)$ [8].

Inelastic scattering is also evident at the commensurate position, $\boldsymbol{\tau}_m = (1, 0, 0)$. This apparent commensurate intensity can be attributed to the finite vertical momentum resolution used in these measurements and the large mosaic of Cr#10, which together lead to significant intensity at $(1, 0, 0)$ from the $(1, 0, \pm\delta)$ silent satellites above and below the scattering plane. These factors also result in an apparently smaller separation between the silent satellite peaks relative to that between the allowed satellite peaks. With the wider vertical resolutions typically employed in previous measurements, these effects lead to the "commensurate diffuse" scattering reported in earlier work [3,4]. To avoid this commensurate contamination and additional intensity normalization problems due to irregular sample geometry, subsequent temperature dependent measurements were performed on the more physically symmetric and mosaically sharper crystal Cr-f.

The temperature dependence of the elastic scattering intensity observed in Cr-f in transverse scans through the allowed $(\pm\delta, 1, 0)$ and silent $(1, \pm\delta, 0)$ satellite positions is shown in the main panel of Fig. 2. The weakly first order transitions at $T_N = 310.3$ K, evident in the allowed satellite data, is characteristic of homogeneous, strain-free chromium. The elastic scattering observed in the silent satellite data indicates that a small fraction of the crystal has ordered with a nesting vector parallel to the (010) axis. The single-**Q** ratio remains constant at 16:1 for all temperatures below T_N.

For quantitative comparison of the inelastic intensities associated with the silent and allowed satellites, corrections must be made to account for this finite single-**Q** ratio. In addition, attention must be paid to the dependence of the effective scattering volume on sample orientation. Measurements of the incoherent scattering intensities near (100) and (010) indicate that the rectangular shape of Cr-f results in well balanced scattering volumes $I_{100}^{\rm incoh}/I_{010}^{\rm incoh} = 0.99(6)$ for these two orientations. The polarization dependence of the elastic magnetic cross section yields another check of the effective scattering volume. In the transversely polarized SDW phase of chromium, this polarization dependence ideally results in an $\mathcal{R}_{\rm elastic} = 2{:}1$ intensity ratio at satellites for which the scattering vector is, respectively, parallel and perpendicular to the nesting vector [9]. The temperature dependence of this ratio is shown in the bottom panel of Fig. 2 for both the allowed (solid circles) and silent (open circles) satellites [10]. The agreement between the data and $\mathcal{R}_{\rm elastic}$ is generally good and improves with increasing temperature as the ordered moment and the accompanying distortive effects of extinction [11] are reduced.

Representative inelastic, $\Delta E = 0.5$ meV, scans through the allowed and silent $(hk0)$ satellites of Cr-f are shown in Fig. 3. At $T = 282$ K ($T_N - 28.3$ K) the observed inelastic scattering is due solely to spin-wave excitations originating at the allowed satellite positions. The weak scattering evident in the silent satellite data is, within error, spin-wave contamination resulting from the 16:1 admixture of allowed and silent domains. The absence of silent satellite dynamics at $T = 0.9T_N$ demonstrates that the scattering which develops at higher temperatures at these satellite positions is entirely due to critical fluctuations associated with the disappearance of the ordered state at T_N. With increasing temperature the silent satellite scattering grows rapidly so that, at $T = 309.75$ K ($T_N - 0.55$ K), the ratio of the allowed silent intensities is approximately 2:1. This behavior is in sharp contrast to the temperature independent, 16:1 elastic scattering ratio of Fig. 2. Finally, at $T = 311$ K ($T_N + 0.7$ K) the silent and allowed satellite intensities are essentially equal as required by the cubic symmetry of the paramagnetic state.

At all temperatures, the longitudinal and transverse date for Cr-f are well described by Lorentzian-squared and Gaussian line shapes, respectively. The additional width evident in the transverse data is an effect of the crystal mosaic. The growth of the silent satellite intensities is accompanied by an increasingly asymmetric line shape as the vertical spectrometer resolution $\Delta q_z = 0.047$ Å^{-1} (FWHM) includes a fraction of the intensity originating at out-of-plane silent satellites, $(1, 0, \pm\delta)$ and $(0, 1, \pm\delta)$. However, the resulting commensurate contamination is much smaller than that observed in measurements of Cr#10 (Fig. 1). By fitting the spectra over a limited range, as shown by the solid lines in the Fig. 3, quantitative difficulties caused by this vertical scattering can be avoided.

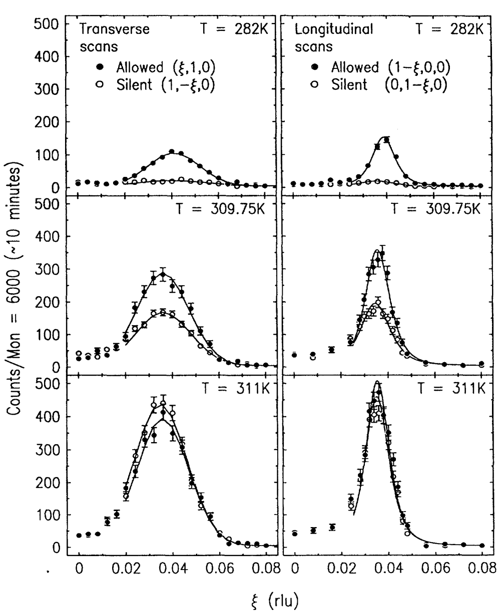

FIG. 3. Inelastic scans with $\Delta E = 0.5$ meV in Cr-f at $T =$ 282, 309.75, and 311 K.

The temperature dependence of the inelastic scattering in Cr-f, corrected for variations due to the $|\mathbf{q}|$ dependence of the magnetic form factor of chromium [10], is shown in Fig. 4. Only spin-wave scattering at the allowed satellite positions is observed at low temperatures. The different intensities of the allowed longitudinal and transverse data reflect an intrinsic spin-wave polarization dependence originally studied as a function of energy by Burke *et al.* [12]. At $T = 282$ K, the ratio of these spin-wave intensities is 1.47(10), somewhat lower than the 1.75 ratio measured by Burke *et al.* at $T = 145$ K. The scattering at all four satellites increases with increasing temperature, with the difference between the allowed and silent satellite intensities remaining roughly equal. This suggests that the fluctuations responsible for the scattering at the silent satellite positions are also present, and of comparable magnitude, at the allowed satellite positions. The equality of the scattering intensities at the longitudinal and transverse silent satellite positions is consistent with critical fluctuations which are *independent* of polarization. At T_N, the scattering at the silent satellites appears to jump discontinuously so that the scattering intensities at all four satellites are, within error, equal in the paramagnetic phase. The inelastic scattering continues to grow above T_N and finally peaks at $T \approx 311$ K ($T_N + 0.7$ K).

The temperature dependence of the FWHM $\mathbf{q}$ width, which provides a measure of the inverse length scale of these fluctuations, is shown in the top panel of Fig. 5. In the paramagnetic phase above T_N the widths of the

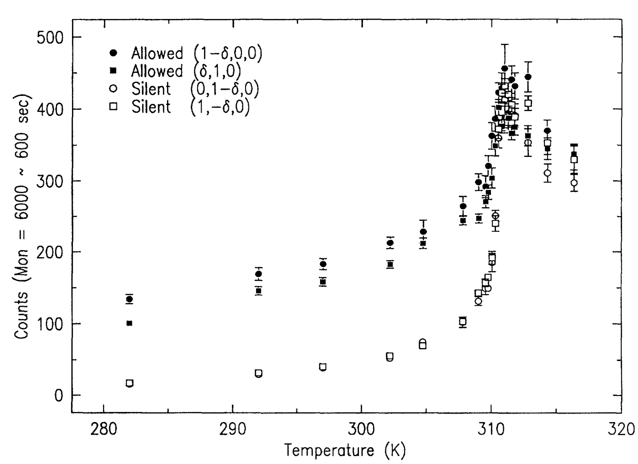

FIG. 4. Temperature dependence of the inelastic intensities with $\Delta E = 0.5$ meV in Cr-f at the four satellite positions in the $(hk0)$ plane.

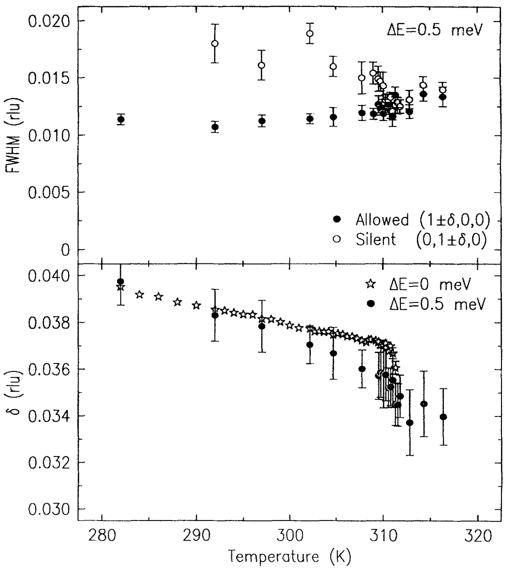

FIG. 5. Top: temperature dependence of the FWHM **q** width of the longitudinal $\Delta E = 0.5$ meV scans in Cr-f. Bottom: temperature dependence of the incommensurability parameter, δ, of the $\Delta E = 0$ and 0.5 meV data.

allowed and silent peaks are approximately equal. With decreasing temperatures below T_N, the silent satellite width grows while the allowed satellite width decreases gradually. The weak minimum in the silent satellite width near T_N indicates that the length scale of the dynamic correlations has, as expected, a maximum near the Néel transition. However, we note that the general temperature evolution of the silent satellite widths, allowing for the weakly first order nature of the transition, does *not* possess a typically critical character as observed, for instance, in localized moment systems.

The temperature dependence of the incommensurability parameter for the elastic $\delta_{0\,\mathrm{meV}}$ and inelastic $\delta_{0.5\,\mathrm{meV}}$ peaks are shown in the bottom panel of the Fig. 5. Well below T_N, $\delta_{0\,\mathrm{meV}}$ decreases in an approximately linear fashion with increasing temperature. However, within a few degrees of T_N this rate of change increases substantially. As the instrumental energy resolution in these measurements is $\delta E = 0.2$ meV (FWHM), these nominally elastic measurements are also sensitive to low energy fluctuations near T_N. The smaller values of $\delta_{0\,\mathrm{meV}}$ at these temperatures, and the slightly smaller values of $\delta_{0.5\,\mathrm{meV}}$ at all temperatures, are consistent with the observation that δ falls off with increasing energy transfers [13]. A more detailed study comparing the energy dependence of delta below and above T_N is currently underway.

The results presented in this paper demonstrate that the commensurate diffuse mechanism invoked in earlier neutron scattering studies has no empirical justification. Rather, the SDW to paramagnetic transition in chromium is driven by critical fluctuations arising at the six satellite positions about the nominal antiferromagnetic zone center: $(1 \pm \delta, 0, 0)$, $(1, \pm\delta, 0)$, and $(1, 0, \pm\delta)$. The common, incommensurate origin of both spin-wave and critical excitations presents a simple and more elegant picture of the magnetic dynamics of chromium. The ability to distinguish critical fluctuations from spin-wave or elastic scattering is a feature unique to the silent satellites of single-**Q** chromium. A superior single-**Q** sample, currently in preparation, should allow a more quantitative and systematic study of the temperature, energy, and **q** dependence of this novel scattering.

We wish to thank Dr. Lawrence G. Rubin of the Francis Bitter National Magnet Laboratory for his help and advice during our efforts to field cool our crystals. Invaluable technical assistance was provided by R. Rothe, J. Biancarosa, and R. J. Liegel. Work at Brookhaven National Laboratory was carried out under Contract No. DE-AC0276CH00016, Division of Materials Science, U.S. Department of Energy. W. T. L. and S. A. W. would like to acknowledge the support of the NSF through Grant No. NSF-PHY 9024608, and E. F. the Natural Sciences and Engineering Council of Canada.

[1] A. Arrott, S. A. Werner, and H. Kendrick, Phys. Rev. Lett. **14**, 1022 (1965).
[2] J. C. R. Fincher, G. Shirane, and S. A. Werner, Phys. Rev. Lett. **43**, 1441 (1979).
[3] J. C. R. Fincher, G. Shirane, and S. A. Werner, Phys. Rev. B **24**, 1312 (1981).
[4] B. H. Grier, G. Shirane, and S. A. Werner, Phys. Rev. B **31**, 2892 (1985).
[5] A. W. Overhauser, Phys. Rev. Lett. **4**, 226 (1960).
[6] T. J. Bastow and R. Street, Phys. Rev. **88**, B935 (1966).
[7] H. B. Møller and A. R. MackIntosh, *Inelastic Scattering of Neutrons* (IAEA, Vienna, 1965), Vol. I, p. 95.
[8] C. F. Eagan and S. A. Werner, Solid State Commun. **16**, 1113 (1975).
[9] After magnetic form factor corrections, see [10].
[10] In longitudinal scans, the amplitudes at $|\mathbf{q}| = 1 - \delta$ and $|\mathbf{q}| = 1 + \delta$ differ due to the **q** dependence of the magnetic form factor. In the elastic data, these two values are averaged for comparison with the transverse intensities. In the inelastic data, the measured intensities are scaled using the form factor **q** dependence extracted from the elastic results.
[11] G. L. Squires, *Introduction to the Theory of Thermal Neutron Scattering* (Cambridge University, Cambridge, England, 1978).
[12] S. K. Burke, W. G. Stirling, K. R. A. Ziebeck, and J. G. Booth, Phys. Rev. Lett. **51**, 494 (1983).
[13] S. K. Burke (private communication); S. A. Werner (unpublished) as cited in [14].
[14] E. Fawcett, Rev. Mod. Phys. **60**, 209 (1988).